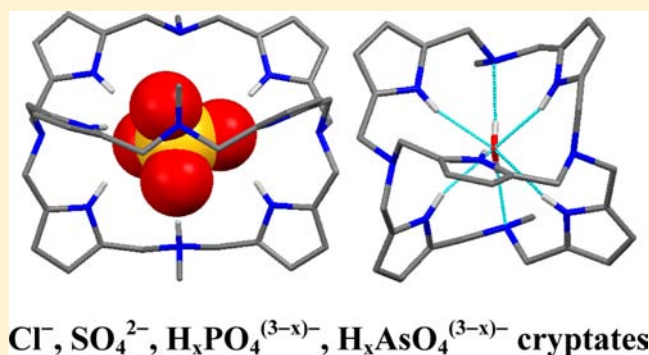


Synthesis of Novel Polyazacryptands for Recognition of Tetrahedral Oxoanions and Their X-ray Structures

Debasish Jana,[†] Ganesan Mani,^{*,†} and Carola Schulzke[‡][†]Department of Chemistry, Indian Institute of Technology-Kharagpur, Kharagpur, West Bengal 721 302, India[‡]Ernst-Moritz-Arndt-Universität Greifswald, Institut für Biochemie, Felix-Hausdorff-Strasse 4, Greifswald 17487, Germany

Supporting Information

ABSTRACT: The Mannich reaction of tris(pyrrolyl- α -methyl)amine (H_3tpa) with a mixture of formaldehyde and primary amine hydrochloride (methyl or ethyl) gave two novel macrobicyclic molecules: a hexapyrrolic pentaazacryptand and an unusual pentapyrrolic tetraazacryptand, which were separated by column chromatography and their structures were determined by X-ray diffraction method. The analogous reaction using benzylamine hydrochloride yielded the encapsulated chloride anion complex in 16% yield even after neutralization with aqueous K_2CO_3 , which was also characterized by X-ray diffraction. In addition, the anion binding properties of these macrobicycles were investigated by NMR titration methods, and the binding constants for halides and oxoanions were determined with the EQNMR program. The cavity of the hexapyrrolic pentaazacryptand is flexible and large enough enabling it to form inclusion complexes with the smaller size fluoride ion as well as with the bulkier oxoanions. This was demonstrated by ^{19}F NMR spectroscopy and by the X-ray structures of the encapsulated sulfate, phosphate, and arsenate ion complexes. Upon complexation the distance between the bridgehead nitrogen atoms changes. Further, anion induced conformational changes were observed in the structures of the oxoanion complexes, particularly in the arsenate structure which represents the first azacryptand encapsulated structure of an arsenate ion. Furthermore, the competition crystallization experiment showed that the phosphate ion complex of the hexapyrrolic pentaazacryptand is the sole crystallization product from an aqueous–organic medium, as confirmed by IR and powder X-ray diffraction studies.



INTRODUCTION

Oxoanions such as sulfate and phosphate are abundantly present in biological and environmental systems and cause both beneficial and deleterious effects to human beings.¹ In nature, the selective recognition and transport of these anions takes place by hydrogen bonding alone as well as in combination with charged peptide units. For example, the sulfate anion is recognized and transported by the sulfate-binding protein merely by means of hydrogen bonding.² Sulfate ions are also present in nuclear fuel waste along with other oxoanions, which eventually end up in the environment.³ On the other hand, the phosphate anion is being recognized and transported by both hydrogen bonds and charged peptide residues. The large quantity of phosphate ions stemming from factories and fertilizers is responsible for causing eutrophication of rivers and ponds, which poses a serious environmental problem.⁴ Another deleterious anion is arsenate, which causes critical and chronic diseases including cancer.⁵ Arsenic is present in soil as arsenite [As(III)] or arsenate [As(V)] contaminating groundwater in many parts of the world, and many people worldwide are exposed to these ions.^{6,7}

In view of this, recognition of anions by synthetic receptors and their coordination chemistry have attracted attention and

remain an active area of research in supramolecular chemistry.⁸ A variety of synthetic receptors have been designed to recognize specific anions with great affinity and selectivity effected by means of interactions such as hydrogen bonding, electrostatic force, or covalent bonding. It is known that the energy of interaction exerted by a synthetic receptor should be large enough to overcome the Gibbs energy of hydration of the anions of interest when seeking selective recognition in an aqueous medium.⁹ Typically neutral hydrogen bonding receptors have been shown to be selective in organic solvents, but not in an aqueous medium. Nevertheless, Kubik and co-workers have demonstrated selective binding of the sulfate anion in an aqueous medium by the neutral cyclopeptide receptors.¹⁰ Moyer, Sessler, Bowman-James, and co-workers have reported the selective extraction of sulfate anions from an aqueous medium by neutral macrocyclic calixpyrrole receptors.¹¹ Gabbai and co-workers have synthesized cationic borane compounds, which very efficiently sense fluoride ions in water.¹²

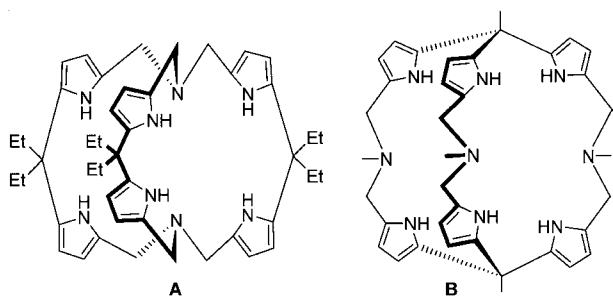
Received: February 6, 2013

Published: May 10, 2013

Under these circumstances, bicyclic receptors are of great importance and have attracted considerable attention as they have optimum suitable size, which can be fine-tuned. With their potentially interacting preorganized groups in the right places, they are consequently potent receptors for the selective recognition of various anions. Indeed, several bicyclic receptors have been shown to possess size selective anion binding properties.¹³ In particular, the tren-based bicyclic receptors bearing bridgehead nitrogen atoms remain a well explored class of bicyclic receptor systems for recognizing anions.¹⁴ For example, some time ago Lehn and co-workers demonstrated the size selective anion binding properties of multiprotonated tris(2-aminoethyl)amine (tren)-based cryptands toward fluoride and azide ions in aqueous media.^{15,16}

In contrast to macrocyclic receptors, reports of macrobicyclic receptor systems based on pyrrole building blocks are so far rather limited.¹⁷ As a continuation of our interests in developing pyrrole-based synthetic receptors for anions, we have been using the Mannich reaction approach for synthesizing novel macrocycles and macrobicycles.^{18,13f,g} Recently, we reported macrobicyclic receptors **A** and **B** (Chart 1) containing both

Chart 1. Bicyclic Pyrrole-Based Receptors Having Relatively Small Cavities and Being Suitable Only for Encapsulating the Comparably Small, Fluoride Ion, Inside Their Cavities



hydrogen bond acceptors and donors with bridgehead nitrogen or carbon atoms which effectively recognize only fluoride ions in the presence of other competing anions in a competitive solvent, while larger ions or oxoanions bind to the clefts of the macrobicyclic.^{13f,g} These results have encouraged us to further explore the Mannich reaction with pyrrole systems to obtain novel macrobicycles possessing suitable cavity sizes for the selective recognition of different oxoanions. Although several synthetic receptors have been reported for the selective recognition of oxoanions,¹⁹ the encapsulation of oxoanions inside the cavity of cryptand-like receptors is more challenging

because it requires not only a size-cavity match between the anion and the receptor with preorganized binding groups, but also the “windows” of the cryptand should be large enough to allow these large anions to get in.⁴ Herein, we report a new class of macrobicyclic pentaaza- and an unusual tetraazacryptand/s synthesized by the Mannich reaction of tris(pyrrolyl- α -methyl)amine and their anion binding properties. The X-ray structures of both the azacryptands and their anion inclusion complexes such as chloride, sulfate, phosphate, and arsenate are discussed in detail. We also report the competition crystallization experiment for selective crystallization of the phosphate ion complex of the pentaazacryptand from an aqueous-organic medium.

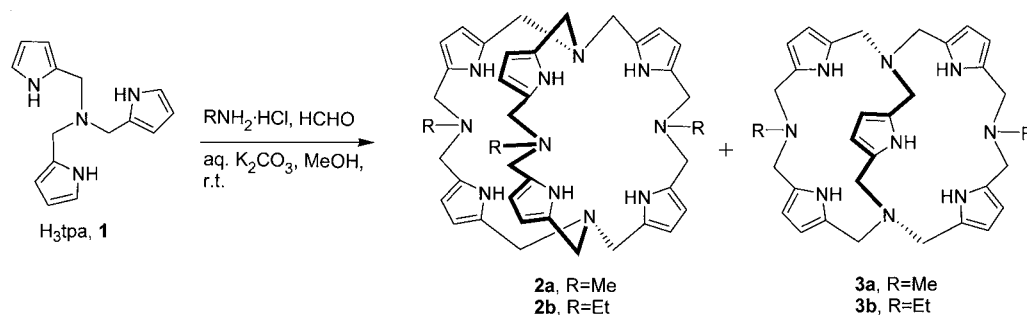
RESULTS AND DISCUSSION

Synthesis and Characterization of the Azacryptands.

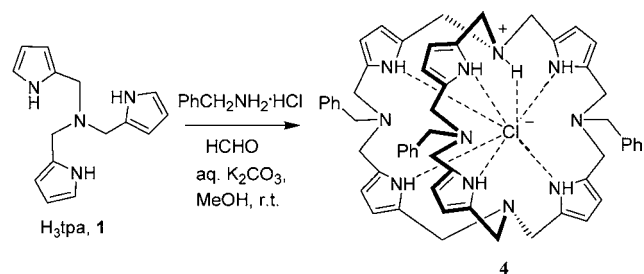
The cavity size of the macrobicyclic molecule **A** or **B** can be enlarged by the Mannich reaction approach with a precursor molecule containing additional spacer units such as the methylene group between the binding sites. By this the macromolecule should become suitable for the selective recognition and encapsulation of larger oxoanions inside its cavity. This hypothesis was investigated using tris(pyrrolyl- α -methyl)amine. Thus, the Mannich reactions of tris(pyrrolyl- α -methyl)amine (H_3tpa) **1** with a mixture of formaldehyde and primary amine hydrochloride (methyl or ethyl) were carried out to give two novel macrobicyclic molecules, **2** and **3**, which were isolated in analytically pure form by basic alumina column chromatography (Scheme 1). The yields for the hexapyrrolic pentaazacryptands **2** are better (22%, Me and 15%, Et) than those (2%, Me and 3%, Et) for the unusual pentapyrrolic tetraazacryptands **3**. While the symmetrical macrobicyclic **2** is the expected target molecule in this reaction, **3** is a rather unexpected macrobicyclic product, which could have formed by the cleavage of one of the $-CH_2(C_4H_4N)$ groups in **1**. Conversely, an analogous reaction using benzylamine hydrochloride gave the chloride ion inclusion complex **4** in 16% yield even after neutralization with an aqueous K_2CO_3 solution instead of the neutral compound that is analogous to **2**; the analogous pentapyrrolic macrobicyclic was not isolated (Scheme 2). The structures of both types of azacryptands **2a** and **3a** and the chloride cryptate **4** were confirmed by single crystal X-ray diffraction and were further supported by solution state spectroscopic data.

The 1H NMR spectra of **2a** and **2b** in $CDCl_3$ show broad singlets at $\delta = 9.50$ and 9.40 ppm for their pyrrolic NH resonances, respectively, suggesting that all NHs are equivalent because of their symmetrical structure. Although **2a** bears two

Scheme 1. Synthesis of Macrobicyclic Receptors by the Mannich Reaction of H_3tpa **1: Hexapyrrolic Pentaazacryptand **2** and Pentapyrrolic Tetraazacryptand **3****



Scheme 2. Synthesis of the Chloride Cryptate 4 Using the Mannich Reaction of H₃tpa 1 with Benzylamine Hydrochloride



types of methylene groups [$\text{N}(\text{CH}_2)_3$ - and MeNCH_2 -], only one broad singlet is observed, which is in contrast to **2b** displaying two separate singlets for its methylene groups. This contrasting feature was settled by the ^{13}C NMR spectra, which showed one signal for each type of methylene group in **2** in CDCl_3 . The pyrrolic NH resonance of **3a** or **3b** appears as two separate broad singlets in the ^1H NMR spectrum because of its unsymmetrical structure. For example, the NH resonances at $\delta = 9.21$ and 10.10 ppm with the integrated intensity ratio of 1:4 are observed for **3a**, just as expected. The presence of three types of CH_2 groups in **3a** and four types in **3b** are supported by the respective ^1H and ^{13}C NMR spectra. The ^1H NMR spectrum of **4** shows three broad resonances with the integrated intensity ratio of 1:3:3 for its three types of NH protons: one ammonium N^+H and two types of three pyrrolic NH groups as expected for this structure. All methylene protons, however, appear as broad signals probably indicating a dynamic process in solution which may render all methylene resonances to be broad signals for the chloride cryptate **4**.

The three-dimensional shape of molecule **2a** was confirmed by X-ray diffraction (Figure 1), and the refinement data are summarized in Table 1. The molecule adopts an eclipsed conformation along the bridgehead nitrogen atoms that resembles the shape of a three-bladed turbine having C_3 symmetry with the lone pairs of the bridgehead nitrogen atoms pointed inside the cavity of the macrobicycle, thus exhibiting an *in-in* configuration. The distance between the bridgehead nitrogen atoms ($\text{N1}\cdots\text{N5}$) is 8.274 \AA and the cavity size is sufficiently large enough to accommodate inside two water molecules, which are H-bonded to five of the six pyrrolic NH groups and the amine nitrogen atoms.

The molecular structure of **3a** is shown in Figure 2. This relatively smaller sized bicyclic molecule can be viewed as the macrocyclic molecule, octahomotetraazacalix[4]pyrrole, strapped by a 2,5-dimethylenepyrrole unit. When viewed along the bridgehead nitrogen atoms, the molecule adopts a tub shape conformation in which one water molecule is bound by hydrogen bonding interactions to four of its five pyrrolic NH groups and two of its four amine groups. This is in contrast to **2a** with two water molecules inside and indicates the presence of a smaller cavity size in **3a** which is supported by the distance between the bridgehead nitrogen atoms ($\text{N1}\cdots\text{N5} = 5.590 \text{ \AA}$) with an *in/in* configuration similar to **2a**.

In the structure of **4**, the presence of one chloride anion inside the cavity of the macrobicycle molecule bearing benzyl groups, which is analogous to **2**, was confirmed by X-ray diffraction (Figure 3). In contrast to the structure of **2a**, in this sphere-shaped molecule **4**, when viewed along the bridgehead nitrogen atoms, only the bridgehead N–C bonds are eclipsed

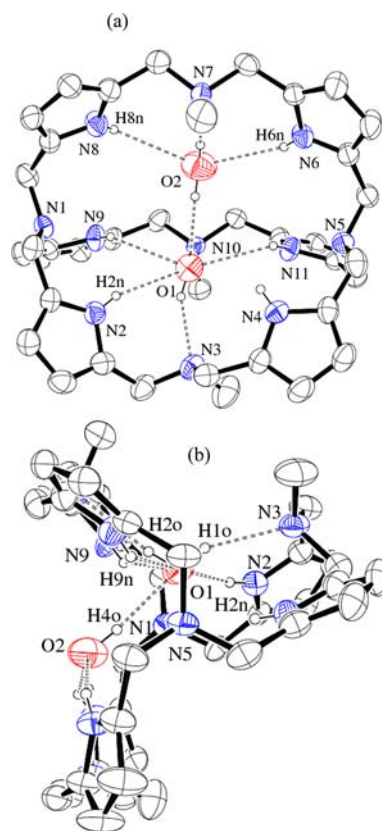


Figure 1. ORTEP diagram of hexapyrrolic pentaazacryptand **2a** (30% thermal ellipsoids): (a) top view and (b) side view. Most hydrogen atoms are omitted for clarity. Selected bond lengths (\AA) and bond angles (deg): $\text{N2}\cdots\text{O1}$, $3.162(6)$; $\text{H2n}\cdots\text{O1}$, $2.36(3)$; $\text{N2}-\text{H2n}\cdots\text{O1}$, $162(5)$; $\text{N8}\cdots\text{O2}$, $3.236(8)$; $\text{H8n}\cdots\text{O2}$, $2.61(5)$; $\text{N8}-\text{H8n}\cdots\text{O2}$, $133(5)$; $\text{N6}\cdots\text{O2}$, $3.227(8)$; $\text{H6n}\cdots\text{O2}$, $2.51(4)$; $\text{N6}-\text{H6n}\cdots\text{O2}$, $146(4)$.

and there is no defined cleft exhibited, probably because of the presence of three sterically hindering benzyl groups at the amine nitrogen atoms; the plane of each benzyl group intersects the bridgehead $\text{N1}\cdots\text{N5}$ vector. The bridgehead nitrogen atom **N5** is protonated and the resultant ammonium cation neutralizes the chloride anion which is hydrogen bonded to all the pyrrolic NH and the ammonium N^+H groups; thus in total there are seven hydrogen bonds involving NH groups to the chloride anion. The chloride anion lies almost in the middle of the vector line connecting the bridgehead nitrogen atoms. The pyrrolic $\text{NH}\cdots\text{Cl}$ distances range from 2.52 to 2.90 \AA and the ammonium $\text{N}^+\text{H}\cdots\text{Cl}$ distance is 2.059 \AA with an $\text{N}^+-\text{H}\cdots\text{Cl}$ angle of 177° suggesting that the chloride anion is bound by rather strong interactions. This hydrogen bonding strength together with the steric protection rendered by the benzyl groups, which “cover up” the three “windows” of the macrobicycle, could enable the molecule to resist an easy removal of the chloride ion from the cavity (K_2CO_3 was used as a base in the synthesis of **4**). On the contrary, in the case of methyl and ethyl derivative reactions (Scheme 1), probably steric protection of these groups to the initially formed chloride ion complex is not sufficient which readily leads to the formation of the neutral macrobicycles **2**. The bridgehead $\text{N1}\cdots\text{N5}$ distance is 6.819 \AA which is shorter than those found for **2a**, and its anion complexes (see below), but it is larger than that reported (6.096 \AA) for the chloride cryptate formed by the thiophene-based azacryptand.²⁰

Table 1. Crystallographic Data for 2a·2H₂O, 3a·H₂O, 4·CH₂Cl₂, [2aH₂]²⁺[SO₄]²⁻ (5), 6, and 7·17.5H₂O

	2a·2H ₂ O	3a·H ₂ O	4·CH ₂ Cl ₂	5	6	7·17.5H ₂ O
empirical formula	C ₃₉ H ₅₃ N ₁₁ O ₂	C ₃₂ H ₄₃ N ₉ O	C ₅₈ H ₆₆ Cl ₃ N ₁₁	C ₃₉ H ₅₃ N ₁₁ O ₄ S	C ₃₉ H ₅₄ N ₁₁ O ₄ P	C ₃₉ H ₈₈ AsN ₁₁ O ₂₁
formula weight	709.94	569.75	1023.57	771.98	771.90	1122.12
wavelength (Å)	0.71073	0.71073	0.71073	0.71073	0.71073	0.71073
temperature (K)	293(2)	293(2)	293(2)	293(2)	293(2)	293(2)
crystal system	monoclinic	triclinic	monoclinic	monoclinic	monoclinic	triclinic
space group	P2 ₁ /c	P $\bar{1}$	P2 ₁ /n	P2 ₁ /n	Cc	P $\bar{1}$
a/Å	13.2379(16)	10.7107(8)	16.024(3)	13.810(4)	22.635(5)	13.0215(12)
b/Å	19.726(2)	11.4969(9)	15.833(3)	15.403(5)	15.677(3)	16.1623(15)
c/Å	15.9349(19)	14.4633(11)	23.489(5)	18.966(6)	11.689(3)	16.6439(15)
α /deg	90.0	99.001(2)	90.0	90.0	90.0	66.874(3)
β /deg	103.309(4)	101.778(2)	109.111(6)	91.868(10)	104.148(10)	67.727(3)
γ /deg	90.0	111.484(2)	90.0	90.0	90.0	67.019(3)
volume (Å ³)	4049.3(8)	1569.2(2)	5631(2)	4032(2)	4022.1(16)	2858.4(5)
Z	4	2	4	4	4	2
D _{calcd} , mg m ⁻³	1.165	1.206	1.207	1.272	1.275	1.304
μ /mm ⁻¹	0.075	0.077	0.210	0.135	0.123	0.673
F(000)	1528	612	2168	1648	1648	1200
θ range (degree)	1.58 to 25.00	1.97 to 25.00	1.58 to 24.62	1.70 to 25.00	1.60 to 26.39	1.38 to 26.26
total/unique no. of reflns.	47512/7099	18659/5499	63822/9466	47523/7106	25110/7527	36590/11296
R _{int}	0.1456	0.0228	0.0807	0.1114	0.1090	0.0723
data/restr./params.	7099/19/500	5499/11/401	9466/0/643	7106/21/531	7527/23/546	11296/24/593
GOF (F ²)	1.028	1.026	0.911	0.980	0.957	0.906
RI, wR2	0.0842, 0.2080	0.0365, 0.0971	0.0580, 0.1435	0.0527, 0.1007	0.0957, 0.2184	0.0697, 0.1778
R indices (all data) RI, wR2	0.2077, 0.2701	0.0479, 0.1069	0.1135, 0.1676	0.1217, 0.1254	0.1555, 0.2458	0.1210, 0.1936
largest different peak and hole (e Å ⁻³)	0.420 and -0.196	0.181 and -0.147	0.168 and -0.148	0.196 and -0.221	0.673 and -0.307	0.647 and -0.391

Anion Binding Studies. The binding properties of 2a and 3a with anions were studied by ¹H NMR titration methods and their binding constants (K_a) were determined with the EQNMR program.²¹ The NMR titration involves addition of an incremental amount of anions in form of their *n*-Bu₄N⁺ salts to the receptor solution in DMSO-*d*₆ or CDCl₃ in an NMR tube and monitoring the change in the NH resonance for calculating apparent binding constants. In the case of the F⁻ ion, the titration spectra showed two NH resonances; one of them appears as a doublet because of the coupling of fluorine with all six NH hydrogen atoms yielding $J(\text{HF}) = 29$ Hz in the deshielded region and corresponds to the fluoride ion complex; the other appears in the shielded region and is due to the free receptor 2a; all this indicates a slow complexation equilibrium process in DMSO-*d*₆ (see Supporting Information, Figure S30). This suggests that the F⁻ ion interacts strongly with the hexapyrrolic macrobicycle 2a by being drawn inside the cavity of the macrobicycle. To confirm that the F⁻ ion is encapsulated, proton coupled ¹⁹F NMR spectra were recorded for 2a in the presence of different mole ratios of F⁻ ions in DMSO-*d*₆. The ¹⁹F NMR spectrum of 2a (Figure 4) with 1 equiv of F⁻ ion showed a septet at $\delta = -91.3$ ppm because of the coupling of the fluoride ion with all six equivalent NH protons yielding the coupling constant $J(\text{HF}) = 29.4$ Hz, which is the same as obtained from ¹H NMR titration spectra, and thus supports the formation of the F⁻ ion inclusion complex in solution. In addition, the spectrum showed multiplets in the shielded region for the formation of F⁻ ion complexes containing deuterium atoms which occur because of the F⁻ ion mediated H/D exchange of the pyrrolic NH hydrogen atoms with DMSO-*d*₆.²² When the mole ratio of F⁻ ion is increased to 2 or 3 equiv, the ¹⁹F NMR spectra showed broad signals corresponding to the

F⁻ ion complexes containing one, two, three, four and five deuterium atoms formed sequentially; the fully deuterium substituted F⁻ ion complex is not observed probably because of the slowness of the H/D exchange (see Supporting Information, Figure S47). The observed broad nature of these signals can be attributed to the formation of a mixture of randomly deuterium substituted F⁻ ion complexes for a given number of deuterium atoms. Further, the ¹⁹F NMR spectrum showed resonances at $\delta = -142.5$ (d) with $J(\text{HF}) = 122$ Hz and at $\delta = -143.0$ (t) with $J(\text{DF}) = 19$ Hz corresponding to the formation of HF₂⁻ and DF₂⁻ species in the solution, respectively, because of H/D exchanges (see Supporting Information, Figure S48). The binding property of 2a with F⁻ ion in a less polar solvent CDCl₃ was also studied by the NMR titration method. In contrast to DMSO, upon addition of F⁻ ions to a CDCl₃ solution of 2a, the NH resonance gradually shifted to the deshielded region, which indicates that all NH groups are cooperatively involved in interacting with this small guest species. However, the titration curve did not achieve a saturation point even after the addition of an excess amount of F⁻ ions (4 equiv) (see Supporting Information, Figure S31). The titration curve is best fitted for a 2:1 rather than 1:1 receptor:anion complex yielding an apparent binding constant K_a of $>10^4$ M⁻² (see Supporting Information, Figure S41). This is in contrast to the titration spectra in DMSO-*d*₆ and suggests that the solvent polarity affects the binding stoichiometry. Further, this 2:1 binding stoichiometry is supported by the Job's plot which shows a maximum around 0.7 mol fraction of receptor, which is close to the expected value of 0.66 mol fraction (see Supporting Information, Figure S45).

The analogous ¹H NMR titration experiment using the smaller macrobicycle 3a with the F⁻ ion was carried out in

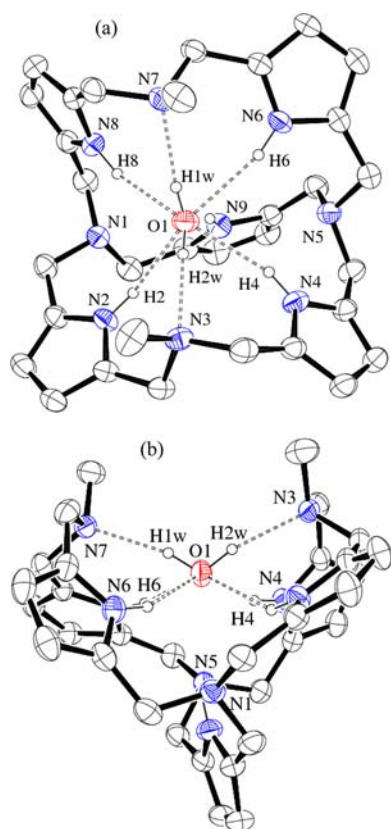


Figure 2. ORTEP diagram of the pentapyrrolic tetraazacryptand **3a** (30% thermal ellipsoids): (a) top view and (b) side view. Most hydrogen atoms are omitted for clarity. Selected bond lengths (Å) and bond angles (deg): N2...O1, 3.0812(16); H2...O1, 2.341(15); N2–H2...O1, 143.1(14); N6...O1, 3.0435(17); H6...O1, 2.193(14); N6–H6...O1, 163.7(15); N3...O1, 2.8458(16); N3...H2w, 1.969(15); O1–H2w...N3, 168.1(16); N7...O1, 2.8478(16); N7...H1w, 1.977(15); O1–H1w...N7, 166.2(16).

CDCl₃, and showed a gradual change and broadening of both of the NH resonances of **3a**. Here again, the titration curve did not reach a saturation point even after addition of 5 equiv of the F[−] ion and was best fitted for the 2:1 stoichiometry (see Supporting Information, Figures S37 and S43) yielding an apparent binding constant K_a of 5029 M^{−2} (<5% error); the 2:1 binding could not be supported by the Job's plot because of the very broad NH resonances. The ¹⁹F NMR spectrum of **3a** with 2 equiv of F[−] ions in DMSO-*d*₆ showed a broad resonance at δ −86.3 ppm for a F[−] ion complex. However, other F[−] ion complexes containing deuterium atoms formed by H/D exchange are not observed although the signals corresponding to HF₂[−] and DF₂[−] species in solution were found (see Supporting Information, Figure S51). The change in the NH resonance upon addition of the larger spherical anions such as Cl[−] and Br[−] to a solution of **2a** or **3a** in CDCl₃ is negligible probably because of comparably weak H-bonding abilities of these anions relative to F[−] and the large cavity size of the receptor which is too voluminous to bind these spherical anions tightly; the determined K_a for **2a** with Cl[−] is <10 M^{−1}.

We then investigated the binding properties of these receptors with bulkier tetrahedral oxoanions. The titration spectra of **2a** with the HSO₄[−] anion in DMSO-*d*₆ appeared to be very complex and showed resonances corresponding to the free receptor and its complex, suggesting a slow complexation equilibrium process (see Supporting Information, Figure S34).

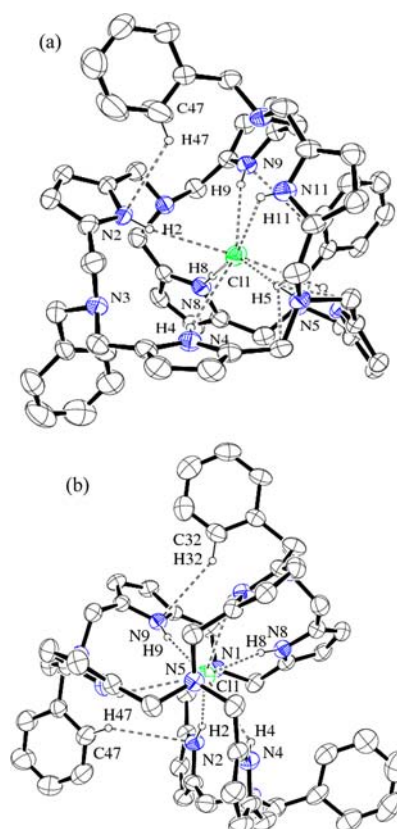


Figure 3. ORTEP diagram of the chloride cryptate **4** (30% thermal ellipsoids): (a) top view and (b) side view. Most hydrogen atoms are omitted for clarity. Selected bond lengths (Å) and bond angles (deg): N2...Cl1, 3.425(3); H2...Cl1, 2.60(3); N2–H2...Cl1, 164(3); N9...Cl1, 3.413(3); H9...Cl1, 2.60(3); N9–H9...Cl1, 169(3); N4...Cl1, 3.477(3); H4...Cl1, 2.79(3); N4–H4...Cl1, 137(3); N5...Cl1, 3.044(2); H5...Cl1, 2.09(3); N5–H5...Cl1, 176(2); N6–Cl1, 3.506(3); H6...Cl1, 2.89(3); N6–H6...Cl1, 133(3); N8–Cl1, 3.404(3); H8...Cl1, 2.52(3); N8–H8...Cl1, 168(3); N11...Cl1, 3.500(3); H11...Cl1, 2.90(3); N11–H11...Cl1, 136(3); C47...N2, 3.659(5); H47...N2, 2.98; C47–H47...N2, 131.5; C32...N9, 3.614(4); H32...N9, 2.84; C32–H32...N9, 141.9.

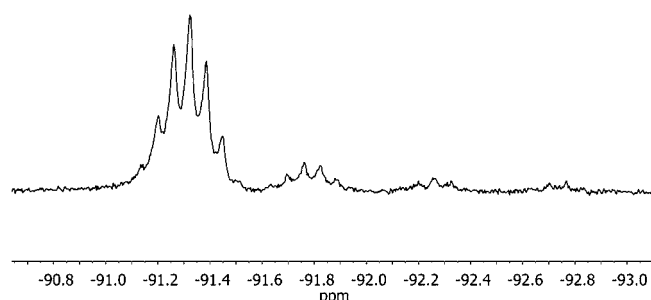


Figure 4. Partial proton coupled ¹⁹F NMR (470.6 MHz) spectrum of the hexapyrrolic pentaazacryptand **2a** (0.008M) with 1 equiv of F[−] ions in the form of the *n*-Bu₄N⁺ salt in DMSO-*d*₆ at 298 K.

The added HSO₄[−] ion could potentially protonate two of the three NMe groups, but not the bridgehead nitrogen atoms as shown by the X-ray structure of the sulfate complex (see below, Figure 5). In the titration spectra, the three resonances appeared as broad overlapped signals in the deshielded region correspond to the pyrrolic NH groups of two types and the ammonium hydrogen atoms (HN⁺Me) of one type. Hence, the

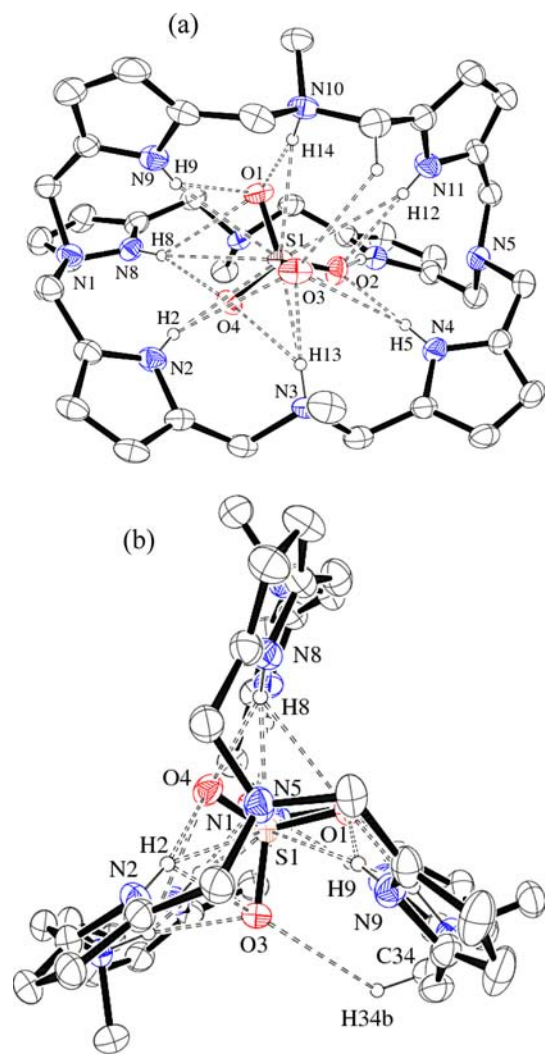


Figure 5. ORTEP diagram of the sulfate anion encapsulated complex **5** (30% thermal ellipsoids): (a) top view and (b) side view. Most hydrogen atoms are omitted for clarity. Selected bond lengths (Å) and bond angles (deg): N2 \cdots O4, 2.882(4); H2 \cdots O4, 2.00(3); N2–H2 \cdots O4, 165(3); N2 \cdots S1, 3.702(3); H2 \cdots S1, 2.88(3); N2–H2 \cdots S1, 152(2); N9 \cdots S1, 3.715(3); H9 \cdots S1, 2.90(3); N9–H9 \cdots S1, 160(3); N4 \cdots O2, 2.833(4); H5 \cdots O2, 1.97(3); N4–H5 \cdots O2, 178(3); N3 \cdots S1, 3.549(3); H13 \cdots S1, 2.69(3); N3–H13 \cdots S1, 161(2); N8 \cdots O4, 2.936(4); H8 \cdots O4, 2.11(3); N8–H8 \cdots O4, 161(3); N6 \cdots O2, 2.820(4); H6 \cdots O2, 1.87(3); N6–H6 \cdots O2, 174(3); N3 \cdots O3, 2.765(3); H13 \cdots O3, 1.88(3); N3–H13 \cdots O3, 167(3); N10 \cdots O1, 2.733(4); H14 \cdots O1, 1.76(3); N10–H14 \cdots O1, 169(3); N11 \cdots O2, 3.050(6); H12 \cdots O2, 2.25(3); N11–H12 \cdots O2 176(3).

binding constant could not be calculated. On the other hand, the titration spectra of **2a** with the HSO_4^- anion in CDCl_3 showed the disappearance of the pyrrolic NH protons before the addition of 1 equiv of HSO_4^- ion, which is probably because of deprotonation of the acidic NH hydrogen atoms (see Supporting Information, Figure S33). The analogous titration spectra of **3a** with HSO_4^- also showed a slow exchange process in CDCl_3 indicating the formation of the sulfate ion complex containing the positively charged receptor in solution. The titration spectra of **2a** with H_2PO_4^- in $\text{DMSO}-d_6$ also showed a slow exchange process indicating that the phosphate anion binds as strongly as the sulfate anion. The analogous titration spectra of **3a** with H_2PO_4^- in CDCl_3 showed a gradual disappearance of the NH resonance because of the depro-

nation with little or no change in the chemical shift position of the NH hydrogens of **3a**, indicating that this pentapyrrole receptor interacts weakly with the H_2PO_4^- ion probably because of a size mismatch. Both receptors showed almost no change in the pyrrolic NH resonance upon addition of NO_3^- ions in the form of its $n\text{-Bu}_4\text{N}^+$ salt in CDCl_3 . This indicates that the NO_3^- ion is not able to form an inclusion complex via hydrogen bonds alone, probably requiring a positively charged receptor as is the case for the SO_4^{2-} and H_2PO_4^- ion complexes.

Crystal Structures of the Oxoanion Complexes. To understand the anion coordination chemistry, binding modes, and conformational changes of the new bicyclic receptor **2a**, the sulfate, phosphate and arsenate anion complexes were synthesized. The sulfate anion complex **5** was obtained in 71% yield as a crystalline solid by the reaction of 2 equiv of $[(n\text{-Bu})_4\text{N}][\text{HSO}_4]$ with **2a** in an ethyl acetate/methanol mixture (Scheme 3). The X-ray structure of the sulfate complex is shown in Figure 5 along with selected bond lengths and angles. The sulfate dianion is encapsulated inside the cavity of the macrobicyclic which adopts an eclipsed conformation with an *in-in* configuration at the bridgehead nitrogen atoms, as in the structure of **2a**. However, the sulfate ion inclusion induces a change in the bridgehead nitrogen distance: N1 \cdots N5 = 8.950 Å, which is longer than that found in the structure of **2a**. The acidic HSO_4^- ion protonates sterically less encumbered NMe groups rather than the sterically crowded bridgehead nitrogen atoms, and the resultant two ammonium cations MeN^+H neutralize the sulfate dianion. Thus the protonated receptor possesses eight potential acidic NH groups (six pyrrolic NH and two ammonium hydrogen atoms) for hydrogen bonding. While each oxygen atom of a sulfate ion can form at least two hydrogen bonds, the sulfate ion in **5** is held tightly in place primarily via bifurcated and trifurcated $\text{NH}\cdots\text{O}$ and $\text{NH}\cdots\text{S}$ hydrogen bond types formed with all of the eight NH groups. However, the oxygen atoms O1, O2, and O4 of the sulfate ion are disordered over two positions indicating that the cavity size of the macrobicyclic is voluminous enough for the sulfate ion to roll around.

The reaction between **2a** and 2 equiv of KH_2PO_4 in THF/water afforded the phosphate cryptate **6** in 77% yield as a crystalline solid (Scheme 3). The X-ray structure (Figure 6) revealed one encapsulated phosphate anion inside the cavity of the pentaazacryptand, and its oxygen atoms are disordered over two positions with several hydrogen bonding interactions. All the pyrrolic NH hydrogen atoms are pointed inside the cavity, and form bifurcated and trifurcated hydrogen bonds with the oxygen atoms of the phosphate anion. The host molecule adopts an eclipsed conformation with an *in-in* configuration, as in the structures of **2a** and **5**, and the distance between the bridgehead nitrogen atoms (N1 and N5) is 9.117 Å, which is longer than those found in the structures of **2a** and **5**. Considering the major component oxygen atoms, the two P–O bond distances (P1–O2 = 1.523(6) Å and P1–O4 = 1.523(6) Å) are shorter than the other two distances, P1–O1 = 1.539(5) Å and P1–O3 = 1.559(6) Å; it may indicate the presence of the monobasic dihydrogenphosphate (H_2PO_4^-) as two of the longer P–O distances could correspond to the protonated oxygen atoms in H_2PO_4^- . These values are longer, though, than the corresponding values reported for the protonated cryptand complex containing an encapsulated H_2PO_4^- anion.²³ However, the positions of hydrogen atoms bound to the bridgehead, the NMe nitrogens or the oxygen atoms of the phosphate anion

Scheme 3. Synthesis of the Oxoanion Encapsulated Complexes of the Hexapyrrolic Pentaazacryptand 2a: Sulfate 5, Phosphate 6, and Arsenate 7 Anion Complexes

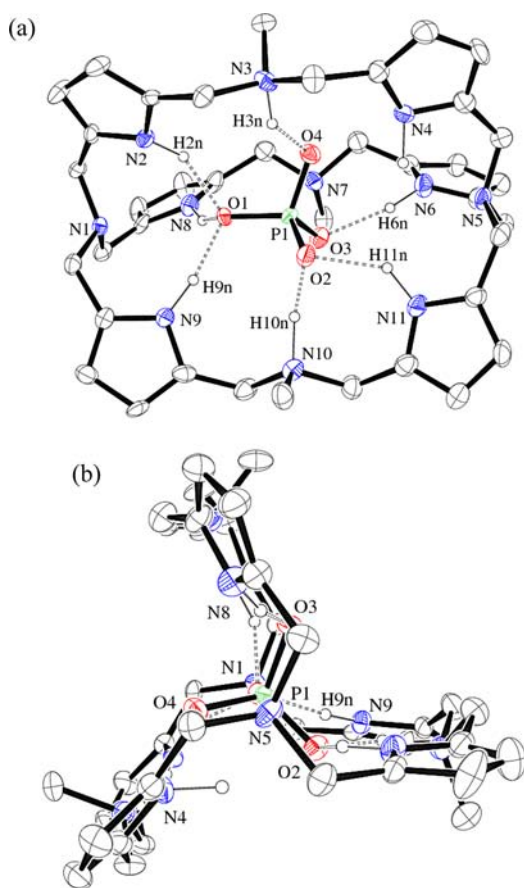
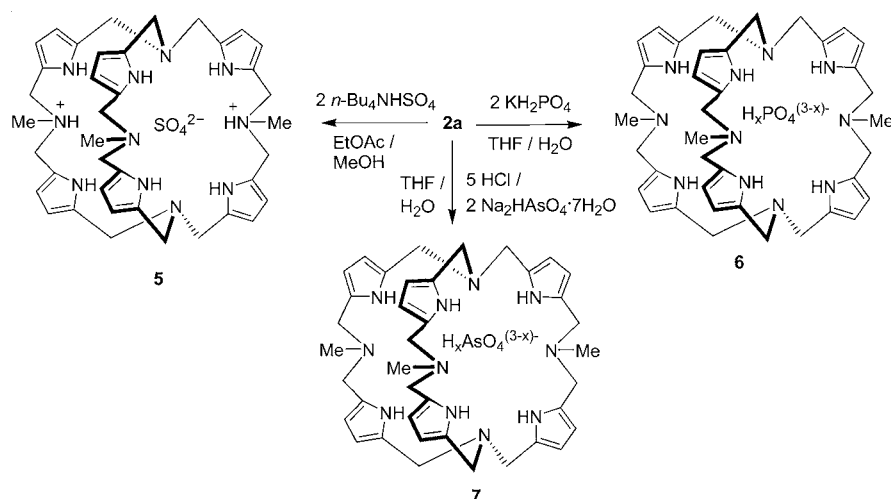


Figure 6. ORTEP diagram of the phosphate anion encapsulated complex 6 (30% thermal ellipsoids): (a) top view and (b) side view. Most hydrogen atoms are omitted for clarity. Selected bond lengths (Å) and bond angles (deg): N1 \cdots O1, 3.066(7); H1n \cdots O1, 1.65(12); N1–H1n \cdots O1, 166(8); N2 \cdots O1, 2.730(8); H2n \cdots O1, 1.74(5); N2–H2n \cdots O1, 148(5); N6 \cdots O3, 2.888(10); H6n \cdots O3, 1.85(5); N6–H6n \cdots O3, 156(7); N7 \cdots O3, 2.628(8); H7n \cdots O3, 1.39(12); N7–H7n \cdots O3, 149(10); N8 \cdots O1, 2.770(8); H8n \cdots O1, 1.73(4); N8–H8n \cdots O1, 157(6); N9 \cdots O1, 2.761(8); H9n \cdots O1, 1.69(4); N9–H9n \cdots O1, 167(7); N10 \cdots O2, 2.589(9); H10n \cdots O2, 1.41(13); N10–H10n \cdots O2, 164(11); N11 \cdots O2, 2.758(8); H11n \cdots O2, 1.86(6); N11–H11n \cdots O2, 137(6).

could not be located exactly as expected. Whether the phosphate species is a neutral H_3PO_4 or trianionic PO_4^{3-} or an intermediate species, to balance the charge, three hydrogen atoms need to be located in the structure. They were found in five positions with an occupancy of roughly 60%. This occupancy was fixed to the value of 0.6 based on four refinement cycles in which the occupancy was set to refine freely and it is in agreement with three hydrogen atoms distributed equally among five positions. In all of the five “cationic” hydrogen atom positions, the hydrogen atoms are located closer to a nitrogen atom rather than to an oxygen atom along hydrogen bonds between the respective N and O atoms. The coordinates of these hydrogen atoms were refined freely, but their displacement factors were set to be dependent on their parent atoms (1.2 times). It needs to be stressed, though, that the data for these five hydrogen atom positions should be taken with caution, since their positions lie along O–N vectors in shallow potential wells. They were refined because electron density was actually observed in suitable positions and because it gives a more comprehensive picture of the hydrogen bonding in the molecule than fixing them in randomly chosen positions or not at all.

The observed two different types of P–O bond lengths may be attributed to partly rather strong hydrogen bonding, as shown by the N \cdots O contacts including strong interactions/short distances such as N10 \cdots O2 = 2.589(9) Å and N \cdots O = 2.628(8) Å. Similar strong hydrogen bonding and ambiguity in hydrogen-locations have been observed in the structures of phosphate anion complexes formed by synthetic receptors before.²⁴ Such strong hydrogen bonding may influence P–O bond lengths significantly. Analogous observations have been made previously.²⁵ Given the disorder and the distribution of hydrogen atoms among the hydrogen bonding atoms within the cavity, it is difficult to assign exactly what type of phosphate anion is present; theoretically it may be any type of phosphate anion structurally lying in between the two extremes, the fully protonated H_3PO_4 and the deprotonated PO_4^{3-} . Overall the actually refined hydrogen atoms represent most likely the average of a mixture of distinct cocrystallized species, reflecting a dynamic proton ping-ponging situation in solution. In any case, this structure represents, to the best of our knowledge, only the second example of a structurally characterized

phosphate anion inclusion complex with a bicyclic azacryptand molecule.²³

We then set to synthesize encapsulation complexes of still larger oxoanions with **2a** for investigating anion induced conformational changes in the macrobicyclic. The reaction of 2 equiv of $\text{Na}_2\text{HAsO}_4 \cdot 7\text{H}_2\text{O}$ with a mixture of **2a** and 5 equiv of HCl in tetrahydrofuran (THF)/water gave the novel inclusion complex **7** containing an arsenate ion in 54% yield as a crystalline solid (Scheme 3). **7** is not formed in the absence of HCl suggesting that a cationic receptor is required for the arsenate ion complex formation. The excess acid used in the synthesis could give a cationic macrobicyclic complex containing a chloride anion which is then replaced by the mono- or dibasic arsenate ion to give **7**. This process is probably driven by the presence of both the hydrogen bond donor and acceptor properties available with the H_2AsO_4^- or HAsO_4^{2-} anion and favored by the suitable cavity size of the macrobicyclic **2a**.

The structure of **7** was determined by X-ray diffraction (Figure 7) and confirmed by the HRMS spectrum which shows a peak m/z at 816.3549 corresponding to its $[\text{M}+\text{H}^+]$ ion. The X-ray structure revealed the presence of an arsenate(V) species inside the cavity of macrobicyclic **2a** along with 17.5 water molecules as cocrystallized solvent in the lattice. The arsenic atom and two of its oxygen atoms (O2 and O4) are disordered over two positions with occupancy factors of 76% and 24% within the cavity of the macrobicyclic. Of overall 3.5 water molecules per formula which could be refined (out of 17.5 in total), half a water molecule (O8) is disordered in correlation with both the disordered methyl group (C33) and the arsenate ion. It appears as if the methyl group can occur as flipped into the macrobicyclic in case the arsenate oxygen atom is not pointing into the same direction (O1 present not O1A). The water (O8) is then hydrogen bonded to the parent nitrogen of this methyl group from outside the cavity. With the minor component of the arsenate disorder present, the methyl group has to be flipped out of the macrocycle for steric reasons. In this case the respective water molecule is apparently hydrogen bonded to the arsenate oxygen and present in the vicinity of the cavity. A third possibility is the presence of the water in this location without the methyl group rotated in and with the arsenate oxygen pointing into the other direction. It appears as if all three possible isomeric structures are cocrystallized. Based on an overall occupancy of only 50% for this water molecule and the additional disorder, the respective water hydrogen atoms could not be located.

In the major component arsenate ion, there are roughly two types of As–O bond distances, as observed in the phosphate complex **6**; As1–O1 (1.671(3) Å) and As1–O4 (1.664(3) Å) are one type, while As1–O2 (1.700(4) Å) and As1–O3 (1.702(3) Å) are the other type. If the former and the latter distances correspond to the nonprotonated and protonated oxygen atoms bound to the arsenic atom in H_2AsO_4^- , respectively, then the difference between the average values of this double and single bond is 0.034 Å. This is not overwhelmingly supporting the presence of the monobasic H_2AsO_4^- anion because this difference is smaller than that found for LiH_2AsO_4 (0.066 Å)²⁶ or $\text{NH}_4\text{H}_2\text{AsO}_4$ (0.05 Å)²⁷ though it roughly falls into this range. On the other hand, if the encapsulated arsenate ion is AsO_4^{3-} with the tripositively charged receptor, then all four As–O bond distances should be almost equal, as found for $(\text{NH}_4)_3\text{AsO}_4$ (1.671 Å, 1.683 Å, 1.686 Å and 1.700 Å)²⁸ or for Cs_3AsO_4 (1.670 Å, 1.670 Å,

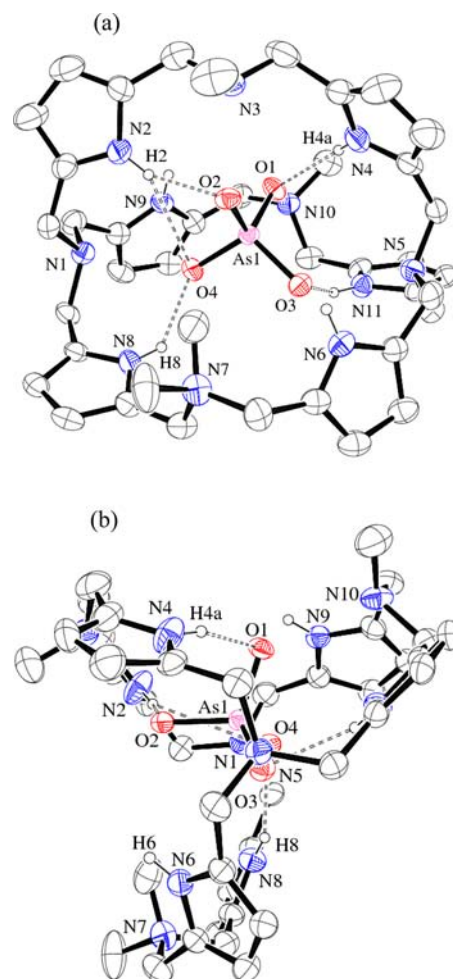


Figure 7. ORTEP diagram of the arsenate anion encapsulated complex **7** (30% thermal ellipsoids): (a) top view and (b) side view. Most hydrogen atoms are omitted for clarity. Selected bond lengths (Å) and bond angles (deg): As1–O1, 1.671(3); As1–O2, 1.700(4); As1–O3, 1.702(3); As1–O4, 1.664(3); O4–As1–O1, 113.40(17); O4–As1–O2, 107.32(18); O1–As1–O2, 109.03(18); O4–As1–O3, 107.41(14); O1–As1–O3, 110.10(17); O2–As1–O3, 109.49(16); C1–N1–C27, 111.1(3); C1–N1–C26, 110.2(3); C27–N1–C26, 110.0(3); C13–N5–C39, 111.5(3); C13–N5–C14, 111.1(3); C39–N5–C14, 109.7(3); C39–N5–N1–C1 = 45.94; C13–N5–N1–C26 = 46.69; C14–N5–N1–C27 = 47.66.

1.679 Å, and 1.689 Å).²⁷ Given these values, even if either AsO_4^{3-} or H_3AsO_4 is present which are the two extremes, location of the hydrogen atoms becomes essential for confirming what type of arsenate ion is present. The counter cationic moiety can be formed by protonation of any of the amine nitrogen atoms of the receptor (HN^+) or by protonation of water to form H_3O^+ , since the arsenate species moves inside the cavity as shown by its disorder. However, the position of any of the neutralizing “protons” (H^+) attached to the arsenate or water oxygen or amine nitrogen atoms could not be precisely located. Residual electron density was found, though, in positions in between the water molecules and the oxygen atoms of arsenate (O1; O1A) pointing toward these water molecules and in suitable distances to the NMe nitrogen atoms of the macrobicyclic (in particular N3 and N10). These hydrogens appear to be distributed between different Lewis basic atoms. Though it is weakly supported by the crystallographic data, that they are in specific locations (NMe,

bridgehead N, As–O[−] and water O functions in particular), in contrast to the structure of **6**, a refinement in these positions even with fractional occupancy did not lead to reasonable results. These three hydrogen atoms have therefore not been refined. This type of disordered hydrogen atoms suggests a strong hydrogen bonding network which includes the cocrystallized waters around the arsenate ion. In support of this, the two of the arsenate oxygen atoms O3 and O4 are almost collinear with the bridgehead nitrogens (N1 and N5) and their distances, N1...O4 = 2.631 Å and N5...O3 = 2.619 Å, indicate strong H-bonds with which the arsenate species is held inside. Besides, the other two oxygen atoms (O1 and O2) of the arsenate species also form strong H-bonds with the NMe and the water molecules as shown by their contacts such as N3...O2 = 2.614 Å, N10...O1 = 2.794 Å, O1...O7(water) = 2.648 Å, and O2...O8(water) = 2.560 Å. Further, it suggests that in solution these hydrogen atoms are moving between the donors and acceptors, or in other words, the positive charge or H⁺ required for neutralizing any arsenate anion is delocalized among the Lewis basic atoms involved in hydrogen bonds. Aside from the more severe disorder, this is overall quite similar to the situation found in the structure of phosphate complex **6**.

Furthermore, this situation suggests that the encapsulated arsenate anion can be neither H₃AsO₄ with a neutral receptor nor AsO₄^{3−} with a tripositively charged receptor, but it may very well be a system in between these two extremes or the structure reflects cocrystallization of all potential species. The As–O bond value can be in between the double and single bond values when the O–H bonds are polarized followed by conjugation, as found in the Cu(II) cryptate reported by McKee, Nelson, and co-workers.²⁵ Polarization of the O–H bond of the arsenate species probably takes place because of the conformational constraints of the receptor with which the arsenate is sitting inside the cavity which offer rather close contacts between the hydrogen donors and the acceptors. Consequently, the observed As–O bond distances can reflect the degree of polarization which can lead to As–O bond lengths lying in between the As=O and As–OH distances, that is, exhibiting partial double bond character, which can be depicted as shown in Figure 8.

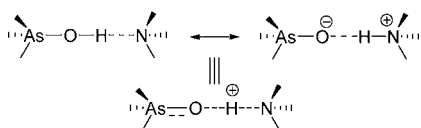


Figure 8. Resonance structures illustrating the delocalization of positive charges between the acceptor and the donor, explaining the distribution of protons among the Lewis basic atoms such as amine, and arsenate or water O atoms in the structure **7** and consequent intermediate As–O distances.

The arsenate ion is held in place via both strong hydrogen bonding as well as electrostatic interactions. The pyrrolic NH groups are H-bonded to the arsenate oxygen atoms and also to the water molecules present in the cleft of the macrobicycle. Importantly, the arsenate anion induces a conformational change from eclipsed, as found in the arsenate free macrobicycle **2a**, to a staggered conformation about the bridgehead N–C bonds with an average torsion angle of 46.76° and an *in/in* configuration at the bridgehead nitrogens. Interestingly, the bridgehead N1...N5 distance of 7.832 Å is considerably shorter than those found in **2a**, **5**, or **6**, although the ionic size of

AsO₄^{3−} is larger than that of the PO₄^{3−} ion,²⁹ indicating a certain flexibility of the macrobicycle's **2a** conformation. A similar distinct property has been observed in the case of the hexaprotonated azacryptand which exhibits a smaller bridgehead N...N distance for the chloride inclusion complex than does its fluoride analogue.³⁰ This structure represents the first arsenate anion inclusion complex with an azacryptand.

It is noteworthy that receptor **2a** is involved in slow exchange processes with anions such as F[−], SO₄^{2−}, and H₂PO₄[−] in DMSO-*d*₆. This led us to investigate which anion binds selectively with **2a** by a competition crystallization method.^{19f,i,18b,31} Thus, when a solution of **2a** in THF/water (1:1 v/v) containing anions such as H₂PO₄[−], HSO₄[−], HAsO₄^{2−}, F[−], Cl[−], Br[−], NO₃[−] (2 equiv each) was allowed to evaporate slowly, only the phosphate complex **6** was formed in 83% yield as a solid. The IR spectrum (see Supporting Information, Figure S53) and the powder XRD pattern (Figure 9) of the precipitate

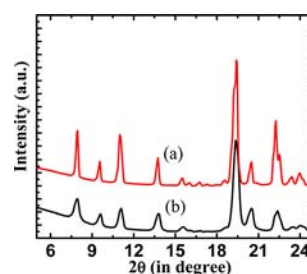


Figure 9. (a) Powder XRD pattern of the phosphate anion complex **6** obtained from its explicit synthesis; (b) the powder XRD pattern of the precipitate obtained from the competition crystallization experiment. The spectrum (a) matches with the spectrum (b), confirming that the phosphate complex is the sole product of crystallization from an aqueous–organic solvent in the presence of other oxoanions.

obtained from the competition experiment are the same as those of **6** obtained from its explicit synthesis. Although it is difficult to confirm the selectivity from this experiment alone because crystallization is a kinetic process and it has to be confirmed from the free energy difference ($\Delta\Delta G$) among other anion complexes,³² it is interesting to note that only the phosphate is crystallized out in the presence of other competing tetrahedral oxoanions; hence, it remains useful for separation of phosphate anions from an aqueous–organic medium. This selective crystallization of the phosphate species is attributed to its hydrogen bond donor and acceptor abilities which complement those present in receptor **2a**. Other competing anions such as SO₄^{2−} or halide anions apparently lack such complementarity.

CONCLUSION

In conclusion, the Mannich reaction approach proved to be an excellent method for synthesizing novel macrobicyclic pentaaza- and tetraazacryptand molecules, which were structurally characterized; the pentaazacryptand **2** is formed by assembling 15 reactive sites in a single step. Interestingly, when bulky benzylamine was used, in contrast to the syntheses of **2** and **3**, a structurally different sphere-like chloride cryptate was isolated. The pentaazacryptand **2a** is a flexible macrobicycle and forms stable inclusion complexes that include the smaller size fluoride ion and the larger size oxoanions, and possesses both hydrogen bonding donors and acceptors with a rather large cavity, as shown by NMR binding and X-ray crystal

structure studies. Further, the competition crystallization experiment in an aqueous–organic medium gave only the phosphate cryptate of **2a**. It is interesting to compare this with the anion binding property of the macrobicycles **A** and **B** in Chart 1 which have been shown to be selective receptors for the smaller fluoride ion in the presence of larger anions which rather bind in their clefts. In contrast to this, this work demonstrated that the cavity size of the macrobicycles can be enlarged using tris(pyrrolyl- α -methyl)amine and the resultant azacryptand possesses additional methylene group spacers so that it becomes suitable for encapsulating larger size oxoanions such as sulfate, phosphate, and arsenate inside the cavity rather than binding in clefts. The inclusion of the arsenate anion inside the cavity of the macrobicycles induces a drastic conformational change to the macrobicycles which is not observed with other anions studied here. The structure of the arsenate complex represents the first structure of an encapsulated arsenate ion inside the cavity of an azacryptand.

EXPERIMENTAL SECTION

Tris(pyrrolyl- α -methyl)amine (H_3tpa) was prepared according to the literature procedure.³⁵ Pyrrole, methylamine hydrochloride, benzylamine hydrochloride, *n*-tetrabutylammonium fluoride solution (1.0 M in THF), *n*-tetrabutylammonium chloride, *n*-tetrabutylammonium bromide, *n*-tetrabutylammonium nitrate, DMSO- d_6 and $CDCl_3$ were purchased from Aldrich and were used without further purification except pyrrole, which was distilled, and methylamine hydrochloride, which was dried under vacuum with warm water. Formaldehyde, *n*-tetrabutylammonium hydrogensulfate, *n*-tetrabutylammonium dihydrogenphosphate, disodium hydrogenarsenate heptahydrate, ethylamine hydrochloride and other reagents were purchased from local commercial sources. 1H NMR (200 and 400 MHz) and ^{13}C NMR (102.6 and 51.3 MHz) spectra were recorded on Bruker spectrometers. Chemical shifts are referenced with respect to the chemical shift of the residual protons present in the deuterated solvents. ^{19}F NMR spectra were recorded on a 500 MHz spectrometer operating at 470.6 MHz for which 0.05% trifluorotoluene in $CDCl_3$ was used as an external reference resonating at -62.72 ppm. FTIR spectra were recorded using Perkin-Elmer Spectrum Rx. High Resolution Mass Spectra (ESI) were recorded using the Xevo G2 Tof mass spectrometer (Waters). Melting points were determined in open capillaries and are corrected using benzophenone as a reference.

Synthesis of 2a and 3a. An aqueous formaldehyde solution (39%, 0.90 mL, 11.7 mmol) was added slowly to a solution of $MeNH_2 \cdot HCl$ (0.40 g, 5.9 mmol) in methanol (700 mL) at 0 °C, and the solution was stirred for 20 min. To this solution at 0 °C, a solution of tris(pyrrolyl- α -methyl)amine (1.0 g, 3.93 mmol) in methanol (50 mL) was added dropwise, and the resultant solution was stirred for 36 h at room temperature. The solvent was removed under vacuum to give an oily residue. Water (80 mL) was added to the residue to give a colorless precipitate. To this reaction mixture, an aqueous solution of K_2CO_3 (0.49 g in 10 mL of water, 3.54 mmol) was added slowly and stirred for about 2 h. The reaction mixture was extracted with dichloromethane (3 \times 25 mL), and the combined organic portion was dried over anhydrous Na_2SO_4 for 4 h. The solvent was removed under vacuum, and the residue was loaded onto a column filled with basic alumina. Elution using a mixture of ethyl acetate/petroleum ether (1:10 v/v) afforded compound **3a** (0.035 g, 2%) as a colorless solid after removal of the solvents. Further elution using ethyl acetate/petroleum ether (1:1 v/v) gave compound **2a** (0.309 g, 22%) as a colorless solid after removal of the solvents.

For **2a**: m.p.: >200 °C. 1H NMR (400 MHz, $CDCl_3$, 25 °C, ppm): δ = 9.50 (br s, 6H, NH), 5.93 (s, 6H, pyrrole β -CH), 5.88 (s, 6H, pyrrole β -CH), 3.51 (s, 24H, CH_2), 1.96 (s, 9H, CH_3). ^{13}C NMR (102.6 MHz, $CDCl_3$, 25 °C): δ = 130.7, 127.1, (pyrrole α -C), 109.2, 107.1, (pyrrole β -C), 55.9, 51.8, (CH_2N), 40.5 ppm (NCH_3). FT-IR (KBr, cm^{-1}): ν = 3372(vs), 3104(w), 2924(w), 2801(s), 1657(w), 1637(w), 1581(w),

1438(s), 1362(w), 1333(w), 1263(w), 1226(w), 1187(w), 1117(w), 1034(w), 1018(w), 971(w), 861(w), 777(vs), 669(w), 650(w), 579(w), 546(w). HRMS(+ESI): m/z calcd for $[M+H]^+$ $C_{39}H_{52}N_{11}$ 674.4402, found 674.4403.

For **3a**: m.p.: >200 °C. 1H NMR (400 MHz, $CDCl_3$, 25 °C, ppm): δ = 10.10 (br s, 4H, pyrrole NH), 9.21 (br s, 1H, pyrrole NH), 5.95–5.87 (m, 10H, pyrrole β -CH), 3.65 (t, 16H, $J(H,H)$ = 12.0 Hz, CH_2), 3.42 (d, 4H, $J(H,H)$ = 12.0 Hz, CH_2), 2.40 (s, 6H, CH_3). ^{13}C NMR (102.6 MHz, $CDCl_3$, 25 °C): δ = 131.0, 130.0, 126.4 (pyrrole α -C), 108.5, 108.0, 105.3 (pyrrole β -C), 54.3, 51.6, 51.2 (CH_2N), 42.7 ppm (NCH_3). FT-IR (KBr, cm^{-1}): ν = 3412(vs), 3376(vs), 3104(w), 2928(w), 2873(w), 2803(vs), 2697(w), 1655(w), 1583(w), 1544(w), 1509(w), 1438(s), 1362(vs), 1278(w), 1259(w), 1226(s), 1178(w), 1116(w), 1035(w), 1013(s), 970(s), 869(w), 785(vs), 697(w), 647(w), 614(w), 573(w). HRMS(+ESI): m/z calcd for $[M+H]^+$ $C_{32}H_{42}N_9$ 552.3558, found 552.3558.

Synthesis of 2b and 3b. **2b** and **3b** were synthesized by following the above procedure for the synthesis of **2a** and **3a**. H_3tpa (0.5 g, 1.96 mmol) was added to the mixture of $EtNH_2 \cdot HCl$ (0.24 g, 2.94 mmol) and HCHO (0.46 mL, 39% aqueous solution, 5.88 mmol) in methanol and stirred for 30 h. **2b** and **3b** were obtained as a colorless solid in 15% (0.105 g) and 3% (0.022 g) yields, respectively, after basic alumina column chromatographic separation which involves elution with ethyl acetate/petroleum ether (1:15 v/v) for **3b** and then with ethyl acetate/petroleum ether (1:3 v/v) for **2b**.

For **2b**: m.p.: >200 °C. 1H NMR (200 MHz, $CDCl_3$, ppm, 25 °C): δ = 9.38 (br s, 6H, NH), 5.88 (d, $J(H,H)$ = 2.0 Hz, 12H, pyrrole β -CH), 3.56 (s, 12H, CH_2), 3.49 (s, 12H, CH_2), 2.45 (q, $J(H,H)$ = 7.1 Hz, 6H, NCH_2CH_3), 0.87 (t, $J(H,H)$ = 7.1 Hz, 9H, NCH_2CH_3). ^{13}C NMR (102.6 MHz, $CDCl_3$, ppm): δ = 130.0, 127.9 (pyrrole α -C), 108.9, 107.5 (pyrrole β -C), 51.9, 51.7 (CH_2N), 46.3 (NCH_2CH_3), 10.0 (NCH_2CH_3). FT-IR (KBr, cm^{-1}): ν = 3388(vs), 3305(s), 3098(w), 2963(w), 2927(w), 2874(w), 2816(s), 2700(w), 1654(w), 1589(w), 1508(w), 1457(w), 1435(w), 1428(w), 1361(s), 1272(s), 1223(w), 1182(w), 1119(w), 1095(w), 1033(s), 971(w), 945(w), 861(w), 775(vs), 665(w), 551(w). HRMS(+ESI): m/z calcd for $[M+H]^+$ $C_{42}H_{58}N_{11}$ 716.4871, found 716.4853.

For **3b**: m.p.: >200 °C. 1H NMR (400 MHz, $CDCl_3$, 25 °C, ppm): δ = 9.94 (br s, 4H, NH), 9.04 (br s, 1H, NH), 5.92–5.86 (m, 10H, pyrrole β -CH), 3.62–3.51 (m, 20H, CH_2), 2.73 (q, $J(H,H)$ = 6.9 Hz, 4H, NCH_2CH_3), 1.10 (t, $J(H,H)$ = 7.2 Hz, 6H, NCH_2CH_3). ^{13}C NMR (102.6 MHz, $CDCl_3$, 25 °C, ppm): δ = 131.1, 130.1, 127.0 (pyrrole α -C), 108.5, 107.9, 105.6 (pyrrole β -C), 51.5, 51.2, 51.2, 48.8 (CH_2N), 10.6 (NCH_2CH_3). FT-IR (KBr, cm^{-1}): ν = 3410(vs), 3367(vs), 3098(w), 2969(w), 2924(w), 2868(w), 2816(s), 2700(w), 1654(w), 1636(w), 1586(w), 1507(w), 1437(w), 1360(s), 1264(s), 1225(w), 1175(w), 1116(s), 1030(s), 968(w), 869(w), 784(s), 763(s). HRMS(+ESI): m/z calcd for $[M+H]^+$ $C_{32}H_{42}N_9$ 580.3871, found 580.3870.

Synthesis of 4. The chloride cryptate **4** was synthesized by following the synthetic procedure of **2a** and **3a**. H_3tpa (2 g, 7.86 mmol) was added to the mixture of $PhCH_2NH_2 \cdot HCl$ (1.69 g, 11.79 mmol) and HCHO (1.81 mL, 39% aqueous solution, 23.6 mmol) in methanol and stirred for 12 h. **4** was isolated in 16% (0.63 g) yield as a colorless solid by using silica gel column chromatography with ethyl acetate/petroleum ether (2:1 v/v) as an eluting solvent. m.p.: >200 °C. 1H NMR (200 MHz, $CDCl_3$, 25 °C, ppm): δ = 11.85 (br s, 1H, N^+H), 10.82, (br s, 3H, pyrrole NH), 9.49 (br s, 3H, pyrrole NH), 7.03–6.81 (m, 15H, aromatic CH), 6.11 (br s, 6H, pyrrole β -CH), 5.84 (br d, 6H, pyrrole β -CH), 5.30 (CH_2Cl_2), 4.13–2.76 (br m, 30H, NCH_2 and $PhCH_2$). ^{13}C NMR (102.6 MHz, $CDCl_3$, 25 °C, ppm): δ = 139.9, 134.8, 131.0, 129.2, 128.4, 126.7 (aromatic C), 116.9, 114.0, 110.7, 106.3 (pyrrole C), 57.4 (CH_2Cl_2), 53.0, 52.5, 52.3, 50.3 (NCH_2). FT-IR (KBr, cm^{-1}): ν = 3372(w), 3323(vs), 3103(w), 3025(w), 2916(w), 2798(w), 2672(w), 2574(w), 1732(w), 1654(w), 1508(w), 1449(w), 1428(w), 1364(s), 1267(w), 1247(w), 1222(w), 1180(w), 1116(w), 1068(w), 1039(w), 1012(w), 973(w), 899(w), 864(w), 776(vs), 742(w), 698(w), 643(w), 579(w), 506(w). HRMS(+ESI): m/z calcd for $[M+H]^+$ $C_{57}H_{65}ClN_{11}$ 938.5113, found 938.5118.

Synthesis of $[2aH_2]^{2+}[SO_4]^{2-}$, 5. To a solution of **2a** (0.025 g, 0.035 mmol) in ethyl acetate (6 mL) was added methanol solution (3

mL) of *n*-Bu₄NHSO₄ (0.024 g, 0.070 mmol) and stirred for 5 min. The resultant solution was allowed to evaporate slowly for 3 days at room temperature to give colorless crystals of **5** which was filtered and dried under vacuum. Yield: 0.019 g, 71%. These crystals are not soluble in organic solvents and hence NMR data could not be obtained. FT-IR (KBr, cm⁻¹): $\nu = 3227$ (vs), 3148(s), 2934(w), 2873(w), 2822(w), 2797(w), 1655(w), 1580(w), 1561(w), 1545(w), 1457(w), 1445(s), 1364(w), 1347(w), 1276(w), 1226(w), 1188(w), 1120(vs), 1092(vs), 1072(vs), 1037(w), 1001(s), 968(w), 868(w), 796(w), 774(s), 617(w). HRMS(+ESI): *m/z* calcd for [M+H⁺] C₃₉H₅₄N₁₁O₄S 772.4075, found 772.4075.

Synthesis of Phosphate Cryptate, 6. To a THF (6 mL) solution of **2a** (0.025 g, 0.035 mmol) was added an aqueous solution (3 mL) of KH₂PO₄ (0.010 g, 0.070 mmol) and stirred for 5 min. The resultant solution was allowed to evaporate slowly for a week at room temperature to give colorless crystals of **6** which was filtered and dried under vacuum. Yield: 0.021 g, 77%. These crystals are not soluble in organic solvents and hence NMR data could not be obtained. FT-IR (KBr, cm⁻¹): $\nu = 3373$ (s), 3188(s), 3091(s), 2969(s), 2812(vs), 2797(vs), 2723(s), 2689(s), 1748(w), 1650(w), 1634(w), 1586(w), 1502(w), 1450(s), 1360(s), 1343(s), 1280(s), 1240(s), 1187(s), 1155(w), 1110(s), 1085(s), 1027(s), 994(vs), 859(s), 785(s), 766(s), 750(s), 690(w), 551(w), 431(w). HRMS(+ESI): *m/z* calcd for [M+H⁺] C₃₉H₅₅N₁₁O₄P 772.4171, found 772.4172.

Synthesis of Arsenate Cryptate, 7·17.5H₂O. To a THF (10 mL) solution of **2a** (0.025 g, 0.035 mmol) was added an aqueous solution of HCl (0.044 mL, 0.175 mmol, 4M) with stirring, resulting in a colorless precipitate. To this solution was added 3 mL of distilled water to dissolve the precipitate to give a clear solution. Then an aqueous solution (2 mL) of disodium hydrogenarsenate heptahydrate (Na₂HAsO₄·7H₂O) (0.021 g, 0.071 mmol) was added and stirred for 5 min. The solution was allowed to evaporate slowly at room temperature over two weeks to give colorless crystals of **7**. Yield: 0.021 g, 0.019, 54%. These crystals are not soluble in organic solvents and hence NMR data could not be obtained. FT-IR (KBr, cm⁻¹): $\nu = 3424$ (vs), 3154(s), 3011(s), 2868(w), 2818(w), 2725(w), 2643(w), 2533(w), 1655(w), 1624(w), 1578(w), 1561(w), 1459(s), 1443(w), 1404(w), 1364(w), 1281(w), 1224(w), 1193(s), 1114(w), 1023(w), 999(w), 903(w), 794(vs), 672(w), 611(w). HRMS (+ESI): calcd *m/z* for [M+H⁺] C₃₉H₅₅AsN₁₁O₄ 816.3649, found 816.3549.

Competition Crystallization. To a THF (14 mL) solution of **2a** (0.025 g, 0.035 mmol) at room temperature was added dropwise 6 mL of aqueous solution containing KH₂PO₄ (0.010 g, 0.070 mmol), Na₂HAsO₄·7H₂O (0.022 g, 0.070 mmol), *n*-Bu₄NHSO₄ (0.024 g, 0.070 mmol), *n*-Bu₄N(NO₃) (0.020 g, 0.070 mmol), *n*-Bu₄NF·3H₂O (0.022 g, 0.070 mmol), *n*-Bu₄NCl (0.019 g, 0.070 mmol), and *n*-Bu₄NBr (0.023 g, 0.070 mmol) with stirring for 10 min and then the solution (pH = 7.60) was allowed to evaporate slowly at room temperature. After 3 days colorless precipitate was formed. The mother liquor was decanted, and the precipitate was washed with water followed by acetone (10 mL) two times and then dried under vacuum. The IR spectrum and the powder XRD diffraction spectrum of this precipitate exactly match with those obtained for the phosphate complex **6**. Yield: 0.022 g, 83%.

NMR Titrations. Using a 10 μ L Hamilton Gastight syringe, all the titrations were carried out by adding an incremental amount of anions as their *n*-tetrabutylammonium salts to the receptor solution in either CDCl₃ or DMSO-*d*₆ (0.008 M, 0.5 mL) in NMR tube. For F⁻, Cl⁻, and Br⁻ anions, the incremental amount is 1 μ L (1 \times 10⁻⁴ mmol, 0.1 equiv) from the 0.4 M stock solution. For HSO₄⁻, H₂PO₄⁻, and NO₃⁻ anions, the incremental amount is 2 μ L (4 \times 10⁻⁴ mmol, 0.1 equiv) from the 0.2 M stock solution. After each addition, the spectrum was recorded and the NH resonance was monitored for calculating the association constants *K*_a by the EQNMR program and other methods.

X-ray Crystallography. Suitable single crystals of **2a** were grown from a solution of **2a** in dichloromethane/petroleum ether (*v/v* = 1:1) upon slow evaporation at room temperature. Suitable single crystals of **3a** and **4** were obtained by layering petroleum ether with a solution of **3a** or **4** in dichloromethane. Suitable single crystals of **5**, **6**, and **7** were obtained from their syntheses.

Single crystal X-ray diffraction data collections for all the compounds were performed at room temperature using Bruker-APEX-II CCD diffractometer with graphite monochromated MoK α radiation ($\lambda = 0.71073$ Å). The structures were solved by SIR-92³⁴ or SHELXS-97 available in WinGX, which successfully located most of the non-hydrogen atoms. Subsequently, least-squares refinements were carried out on *F*² using SHELXL-97 (WinGX version)³⁵ to locate the remaining non-hydrogen atoms.

Typically for all the structures, hydrogen atoms attached to carbons were fixed in calculated positions. The NH and water hydrogen atoms were located, refined isotropically with their thermal parameters set as equivalent to 1.2 times that of their parent atoms and restrained with SADI or DFIX. In case of the structure of **4**, the unit cell contains roughly one molecule of dichloromethane which has been treated as a diffuse contribution to the overall scattering without specific atom positions by SQUEEZE/PLATON.³⁶ The presence of dichloromethane is supported by the ¹H NMR spectrum recorded for crystals of **4** in CDCl₃ showing a singlet at δ 5.30 ppm. In case of the structure of **5**, the oxygen atoms (O1, O2, and O4) of the sulfate anion are found to be disordered over two positions with occupancy factors of 88% and 12% which are handled successfully with EADP and SADI options. In case of the structure of **6**, the phosphate ion is found to be disordered over two positions with occupancy factors of 79% and 21%. The minor component was refined isotropically. The three counter charge hydrogen atoms in total were found to be distributed among five NMe nitrogen atoms. They were located and refined isotropically with 0.6 occupancy factors each. In case of the structure of **7**, the unit cell contains 17.5 water molecules per formula; 14 of them were treated as a diffuse contribution to the overall scattering without specific atom positions by SQUEEZE/PLATON. The remaining 3.5 water molecules were refined. For those with hydrogen atoms that could be located, the hydrogen atoms were located and refined isotropically with their thermal parameters set to being equivalent to 1.5 times that of the parent, and restrained with DFIX to become stable. Half a water molecule is disordered over two positions in correlation with the arsenate disorder. The minor component oxygen atom was refined isotropically. The respective hydrogen atoms could not be found. The arsenic atom and two of its oxygen atoms (O1 and O4) are disordered over two positions with occupancy factors of 76% and 24%. Similarly, the methyl group attached to N7 atom was found to be disordered with occupancy factors of 44% and 56%. The counter charge hydrogen atoms could not be refined with a reasonable result but are part of the calculated sum formula. Use of SQUEEZE/PLATON necessarily contributes to the discrepancy between calculated and reported formulas in the cif-files for the structure of arsenate **7** and chloride complex **4**. The refinement data for all the structures are summarized in Table 1.

■ ASSOCIATED CONTENT

📄 Supporting Information

NMR, IR, binding constant calculations and graphs, crystallographic data (CIF). This material is available free of charge via the Internet at <http://pubs.acs.org>.

■ AUTHOR INFORMATION

✉ Corresponding Author

*E-mail: gmani@chem.iitkgp.ernet.in. Fax: +91 3222 282252.

Notes

The authors declare no competing financial interest.

■ ACKNOWLEDGMENTS

We thank the CSIR and DST (New Delhi, India) for financial support and for the X-ray and NMR facilities. We thank Dr. Swadhin Mandal, Indian Institute of Science Education and Research, Kolkata, for ¹⁹F NMR spectra.

REFERENCES

- (1) (a) Sessler, J. L.; Gale, P. A.; Cho, W.-S. *Anion Receptor Chemistry*; Royal Society of Chemistry: Cambridge, U.K., 2006. (b) Bianchi, A.; Bowman-James, K.; García-España, E. *Supramolecular Chemistry of Anions*; Wiley-VCH: New York, 1997. (c) Katayev, E. A.; Ustynyuk, Y. A.; Sessler, J. L. *Coord. Chem. Rev.* **2006**, *250*, 3004–3037.
- (2) (a) Pflugrath, J. W.; Quioco, F. A. *Nature* **1985**, *314*, 257–260. (b) Pflugrath, J. W.; Quioco, F. A. *J. Mol. Biol.* **1988**, *200*, 163–180.
- (3) (a) Moyer, B. A.; Custelcean, R.; Hay, B. P.; Sessler, J. L.; Bowman-James, K.; Day, V. W.; Kang, S.-O. *Inorg. Chem.* **2013**, *52*, 3473–3490. (b) Moyer, B. A.; Delmau, L. H.; Fowler, C. J.; Ruas, A.; Bostick, D. A.; Sessler, J. L.; Katayev, E.; Pantos, G. D.; Llinares, J. M.; Hossain, M. A.; Kang, S. O.; Bowman-James, K. *Advances in Inorganic Chemistry*; Academic Press: New York, 2006; Vol 59, pp 175–204.
- (4) Bazzicalupi, C.; Bencini, A.; Lippolis, V. *Chem. Soc. Rev.* **2010**, *39*, 3709–3728.
- (5) Hughes, M. F. *Toxicol. Lett.* **2002**, *133*, 1–16.
- (6) (a) Nordstrom, D. K. *Water Sci.* **2002**, *296*, 2143–2144. (b) Greven, M.; Green, S.; Robinson, B.; Clothier, B.; Vogeler, I.; Agnew, R.; Neal, S.; Sivakumaran, S. *Water Sci. Technol.* **2007**, *56*, 161–168.
- (7) Yusof, A. M.; Malek, N. A. N. *J. Hazard. Mater.* **2009**, *162*, 1019–1024.
- (8) (a) Beer, P. D.; Gale, P. A. *Angew. Chem., Int. Ed.* **2001**, *40*, 486–516. (b) Wenzel, M.; Hiscock, J. R.; Gale, P. A. *Chem. Soc. Rev.* **2012**, *41*, 480–520. (c) Bowman-James, K. *Acc. Chem. Res.* **2005**, *38*, 671–678. (d) McKee, V.; Nelson, J.; Town, R. M. *Chem. Soc. Rev.* **2003**, *32*, 309–325. (e) Choi, K.; Hamilton, A. D. *Coord. Chem. Rev.* **2003**, *240*, 101–110. (f) Filby, M. H.; Steed, J. W. *Coord. Chem. Rev.* **2006**, *250*, 3200–3218. (g) Joyce, L. A.; Shabbir, S. H.; Anslyn, E. V. *Chem. Soc. Rev.* **2010**, *39*, 3621–3632. (h) Dydio, P.; Lichosyt, D.; Jurczak, J. *Chem. Soc. Rev.* **2011**, *40*, 2971–2985. (i) Hargrove, A. E.; Nieto, S.; Zhang, T.; Sessler, J. L.; Anslyn, E. V. *Chem. Rev.* **2011**, *111*, 6603–6782. (j) Gale, P. A. *Chem. Commun.* **2011**, *47*, 82–86.
- (9) (a) Schmidtchen, F. P.; Berger, M. *Chem. Rev.* **1997**, *97*, 1609–1646. (b) Schmidtchen, F. P. *Chem. Soc. Rev.* **2010**, *39*, 3916–3935. (c) Kubik, S. *Chem. Soc. Rev.* **2010**, *39*, 3648–3663.
- (10) (a) Kubik, S.; Kirchner, R.; Nolting, D.; Seidel, J. *J. Am. Chem. Soc.* **2002**, *124*, 12752–12760. (b) Kubik, S.; Goddard, R.; Kirchner, R.; Nolting, D.; Seidel, J. *Angew. Chem., Int. Ed.* **2001**, *40*, 2648–2651.
- (11) (a) Fowler, C. J.; Haverlock, T. J.; Moyer, B. A.; Shriver, J. A.; Gross, D. E.; Marquez, M.; Sessler, J. L.; Hossain, M. A.; Bowman-James, K. *J. Am. Chem. Soc.* **2008**, *130*, 14386–14387. (b) Moyer, B. A.; Sloop, F. V., Jr.; Fowler, C. J.; Haverlock, T. J.; Kanga, H.-A.; Delmau, L. H.; Bau, D. M.; Hossain, M. A.; Bowman-James, K.; Shriver, J. A.; Bill, N. L.; Gross, D. E.; Marquez, M.; Lynch, V. M.; Sessler, J. L. *Supramol. Chem.* **2010**, *22*, 653–671.
- (12) Kim, Y.; Gabbai, F. P. *J. Am. Chem. Soc.* **2009**, *131*, 3363–3369.
- (13) (a) Dietrich, B.; Viout, P.; Lehn, J.-M. *Macrocyclic Chemistry*; VCH: Weinheim, Germany, 1993. (b) Amendola, V.; Fabbrizzi, L.; Mangano, C.; Pallavicini, P.; Poggi, A.; Taglietti, A. *Coord. Chem. Rev.* **2001**, *219*–221, 821–837. (c) Ballester, P. *Chem. Soc. Rev.* **2010**, *39*, 3810–3830. (d) Kang, S. O.; Llinares, J. M.; Day, V. W.; Bowman-James, K. *Chem. Soc. Rev.* **2010**, *39*, 3980–4003. (e) Fabbrizzi, L. *Top. Curr. Chem.* **2012**, *323*, 127–166. (f) Guchhait, T.; Mani, G. *J. Org. Chem.* **2011**, *76*, 10114–10121. (g) Guchhait, T.; Mani, G.; Schulzke, C.; Anoop, A. *Inorg. Chem.* **2012**, *51*, 11635–11644.
- (14) (a) Amendola, V.; Bonizzoni, M.; Esteban-Gomez, D.; Fabbrizzi, L.; Licchelli, M.; Sancenon, F.; Taglietti, A. *Coord. Chem. Rev.* **2006**, *250*, 1451–1470. (b) Kang, S. O.; Hossain, M. A.; Powell, D.; Bowman-James, K. *Chem. Commun.* **2005**, 328–330. (c) Das, M. C.; Ghosh, S. K.; Bharadwaj, P. K. *Dalton Trans.* **2009**, 6496–6506. (d) Mateus, P.; Delgado, R.; Groves, P.; Campos, S. R. R.; Baptista, A. M.; Brandão, P.; Félix, V. *J. Org. Chem.* **2012**, *77*, 6816–6824. (e) Arunachalam, M.; Suresh, E.; Ghosh, P. *Tetrahedron* **2007**, *63*, 11371–11376. (f) Mateus, P.; Delgado, R.; Brandão, P.; Félix, V. *J. Org. Chem.* **2012**, *77*, 4611–4621. (g) Chen, D.; Martell, A. E. *Tetrahedron* **1991**, *47*, 6895–6902.
- (15) (a) Dietrich, B.; Lehn, J.-M.; Guilhem, J.; Pascard, C. *Tetrahedron Lett.* **1989**, *30*, 4125–4128. (b) Reilly, S. D.; Khalsa, G. R. K.; Ford, D. K.; Brainard, J. R.; Hay, B. P.; Smith, P. H. *Inorg. Chem.* **1995**, *34*, 569–575. (c) Dietrich, B.; Dilworth, B.; Lehn, J.-M.; Souchez, J.-P.; Cesario, M.; Guilhem, J.; Pascard, C. *Helv. Chim. Acta* **1996**, *79*, 569–587.
- (16) (a) Lehn, J.-M.; Sonveaux, E.; Willard, A. K. *J. Am. Chem. Soc.* **1978**, *100*, 4914–4916. (b) Dietrich, B.; Guilhem, J.; Lehn, J.-M.; Pascard, C.; Sonveaux, E. *Helv. Chim. Acta* **1984**, *67*, 91–104.
- (17) (a) Bucher, C.; Zimmerman, R. S.; Lynch, V.; Sessler, J. L. *J. Am. Chem. Soc.* **2001**, *123*, 9716–9717. (b) Bucher, C.; Zimmerman, R. S.; Lynch, V.; Sessler, J. L. *Chem. Commun.* **2003**, 1646–1647. (c) Cafeo, G.; Colquhoun, H. M.; Cuzzola, A.; Gattuso, M.; Kohnke, F. H.; Valenti, L.; White, A. J. P. *J. Org. Chem.* **2010**, *75*, 6263–6266. (d) Setsune, J.; Watanabe, K. *J. Am. Chem. Soc.* **2008**, *130*, 2404–2405. (e) Fox, O. D.; Rolls, T. D.; Drew, M. G. B.; Beer, P. D. *Chem. Commun.* **2001**, 1632–1633. (f) Francesconi, O.; Ienco, A.; Moneti, G.; Nativi, C.; Roelens, S. *Angew. Chem., Int. Ed.* **2006**, *45*, 6693–6696.
- (18) (a) Mani, G.; Jana, D.; Kumar, R.; Ghorai, D. *Org. Lett.* **2010**, *12*, 3212–3215. (b) Mani, G.; Guchhait, T.; Kumar, R.; Kumar, S. *Org. Lett.* **2010**, *12*, 3910–3913. (c) Kumar, R.; Guchhait, T.; Mani, G. *Inorg. Chem.* **2012**, *51*, 9029–9038.
- (19) (a) Mateus, P.; Delgado, R.; Brandão, P.; Carvalcho, S.; Félix, V. *Org. Biomol. Chem.* **2009**, *7*, 4661–4673. (b) Bazzicalupi, C.; Bencini, A.; Puccioni, S.; Valtancoli, B.; Gratteri, P.; Garau, A.; Lippolis, V. *Chem. Commun.* **2012**, *48*, 139–141. (c) Tobey, S. L.; Jones, B. D.; Anslyn, E. V. *J. Am. Chem. Soc.* **2003**, *125*, 4026–4027. (d) Mendy, J. S.; Pilate, M. L.; Horne, T.; Day, V. W.; Hossain, M. A. *Chem. Commun.* **2010**, *46*, 6084–6086. (e) Mateus, P.; Delgado, R.; Brandão, P.; Félix, V. *J. Org. Chem.* **2009**, *74*, 8638–8646. (f) Yin, Z.; Zhang, Y.; He, J.; Cheng, J.-P. *Tetrahedron* **2006**, *62*, 765–770. (g) Bazzicalupi, C.; Bencini, A.; Giorgi, C.; Valtancoli, B.; Lippolis, V.; Perra, A. *Inorg. Chem.* **2011**, *50*, 7202–7216. (h) Custelcean, R.; Bock, A.; Moyer, B. A. *J. Am. Chem. Soc.* **2010**, *132*, 7177–7185. (i) Dey, S. K.; Das, G. *Dalton Trans.* **2012**, *41*, 8960–8972.
- (20) Saeed, M. A.; Fronczek, F. R.; Hossain, M. A. *Chem. Commun.* **2009**, 6409–6411.
- (21) Hynes, M. J. *J. Chem. Soc., Dalton Trans.* **1993**, 311–312.
- (22) (a) Kang, S. O.; VanderVelde, D.; Powell, D.; Bowman-James, K. *J. Am. Chem. Soc.* **2004**, *126*, 12272–12273. (b) Wang, Q.-Q.; Day, V. W.; Bowman-James, K. *J. Am. Chem. Soc.* **2013**, *135*, 392–399. (c) Chmielewski, M. J.; Jurczak, J. *Chem.—Eur. J.* **2005**, *11*, 6080–6094.
- (23) Yang, L.-Z.; Li, Y.; Jiang, L.; Feng, X.-L.; Lu, T.-B. *CrystEngComm* **2009**, *11*, 2375–2380.
- (24) (a) Nation, D. A.; Reibenspies, J. H.; Martell, A. E. *Inorg. Chem.* **1996**, *35*, 4597–4603. (b) Kral, V.; Furuta, H.; Shreder, K.; Lynch, V.; Sessler, J. L. *J. Am. Chem. Soc.* **1996**, *118*, 1595–1607. (c) Bianchi, A.; Escuder, B.; Fusi, V.; Garcia-España, E.; Giorgi, G.; Marcelino, V.; Paoletti, P.; Valtancoli, B. *J. Am. Chem. Soc.* **1999**, *121*, 6807–6815. (d) Gerasimchuk, O. A.; Mason, S.; Llinares, J. M.; Song, M. P.; Alcock, N. W.; Bowman-James, K. *Inorg. Chem.* **2000**, *39*, 1371–1375. (e) Saeed, M. A.; Pramanik, A.; Hossain, M. A. *Inorg. Chem. Commun.* **2012**, *21*, 32–34.
- (25) Farrell, D.; Harding, C. J.; McKee, V.; Nelson, J. *Dalton Trans.* **2006**, 3204–3211.
- (26) Fanchon, E.; Vicat, J.; Qui, D. T.; Boudjada, A. *Acta Crystallogr., Sect. C* **1987**, *43*, 1022–1025.
- (27) Mähler, J.; Persson, I.; Herbert, R. B. *Dalton Trans.* **2013**, *42*, 1364–1377.
- (28) Hseu, T. H.; Lu, T. H. *Acta Crystallogr., Sect. B* **1977**, *33*, 3947–3949.
- (29) Tawfik, D. S.; Viola, R. E. *Biochemistry* **2011**, *50*, 1128–1134.
- (30) Hossain, M. A.; Llinares, J. M.; Miller, C. A.; Seib, L.; Bowman-James, K. *Chem. Commun.* **2000**, 2269–2270.
- (31) Custelcean, R.; Sellin, V.; Moyer, B. A. *Chem. Commun.* **2007**, 1541–1543.
- (32) Ursu, A.; Schmidtchen, F. P. *Angew. Chem., Int. Ed.* **2012**, *51*, 242–246.

- (33) Shi, Y.; Cao, C.; Odom, A. L. *Inorg. Chem.* **2004**, *43*, 275–281.
- (34) Altomare, A.; Cascarano, G.; Giacovazzo, C.; Guagliardi, A. J. *Appl. Crystallogr.* **1993**, *26*, 343–350.
- (35) (a) Sheldrick, G. M. *Acta Crystallogr.* **2008**, *A64*, 112–122.
- (b) Farrugia, L. J. *Appl. Crystallogr.* **1999**, *32*, 837–838.
- (36) van der Sluis, P.; Spek, A. L. *Acta Crystallogr., Sect. A* **1990**, *46*, 194–201.